

### 3.1 Satellite image processing

#### 1. Akjoujt LANDSAT image processing

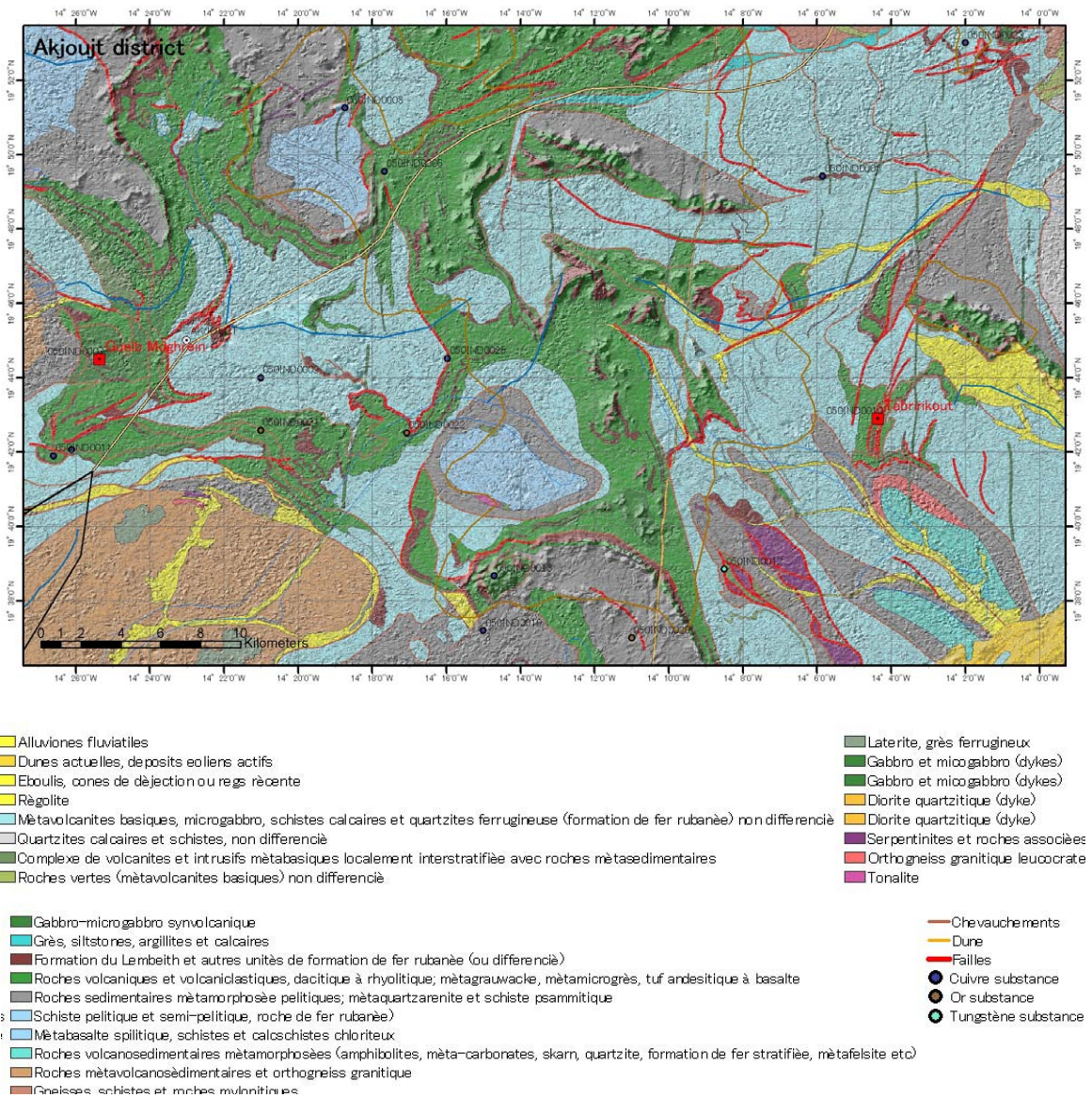


Figure 1 Geology map of the Akjoujt area (after 1:200,000 series, SIGM database)



Figure 2 LANDSAT ETM Infra-red image: vegetation shows as red-pink. Area 1 = Akjoujt Cu-Au Mine; 2 = Tabrinkout tungsten anomaly. Arrows show look-direction of photos below.



Figure 3 Akjoujt Mine: looking west from residual hill / gossan, along the strike of the mineralised metacarbonate and main shear zones.



Figure 4 View north from mine towards Akjoujt hills, treatment plant, tailings dam pond and town reservoir in middle distance.



Figure 5 Looking SW from the meta-carbonate of the Tabrinkout tungsten anomaly (view along old sample trench)

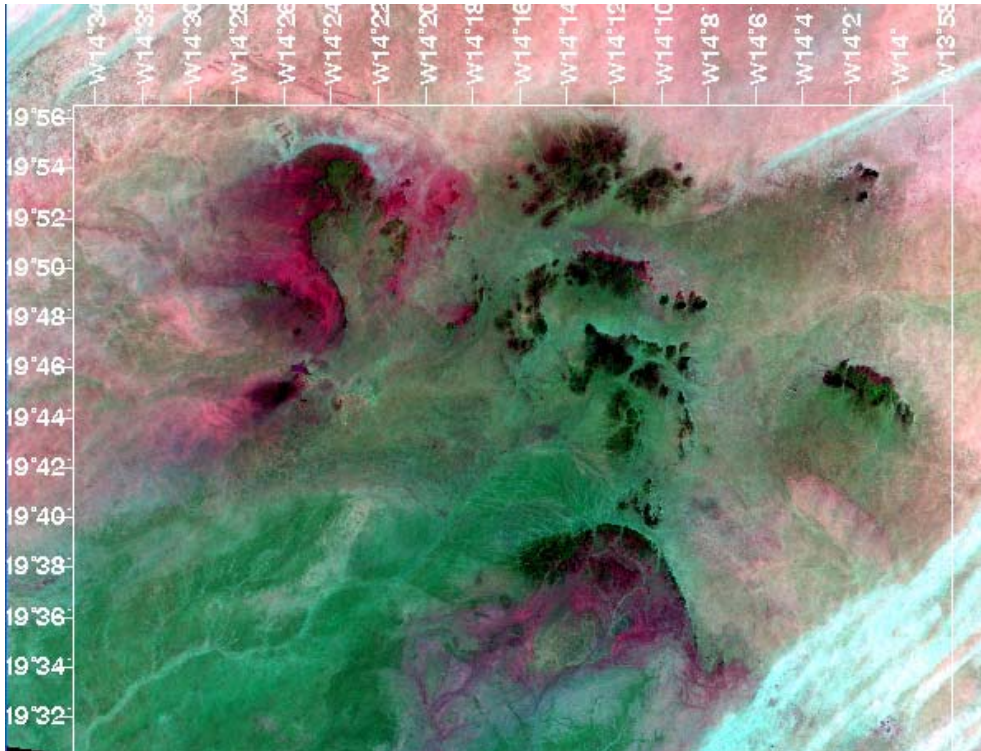


Figure 6 LANDSAT TM\_731\_RGB Pink = granite/migmatite;  
 White-blue = quartz-rich; dark brown-ruby red = BIF & debris  
 Green = schists & meta-carbonates

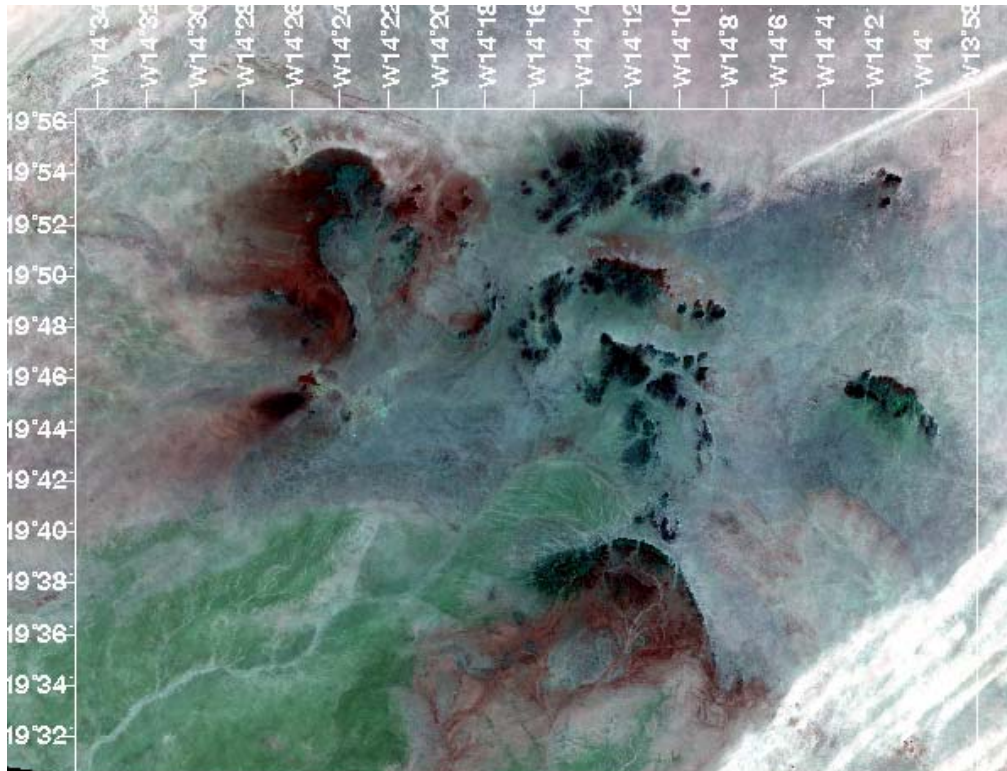


Figure 7 LANDSAT TM\_(351)(517)(741)\_RGB Pale blue = chlorite schists, dark grey lenses within the chlorite schists are meta-carbonates. Green in SW corner = orthogneiss?

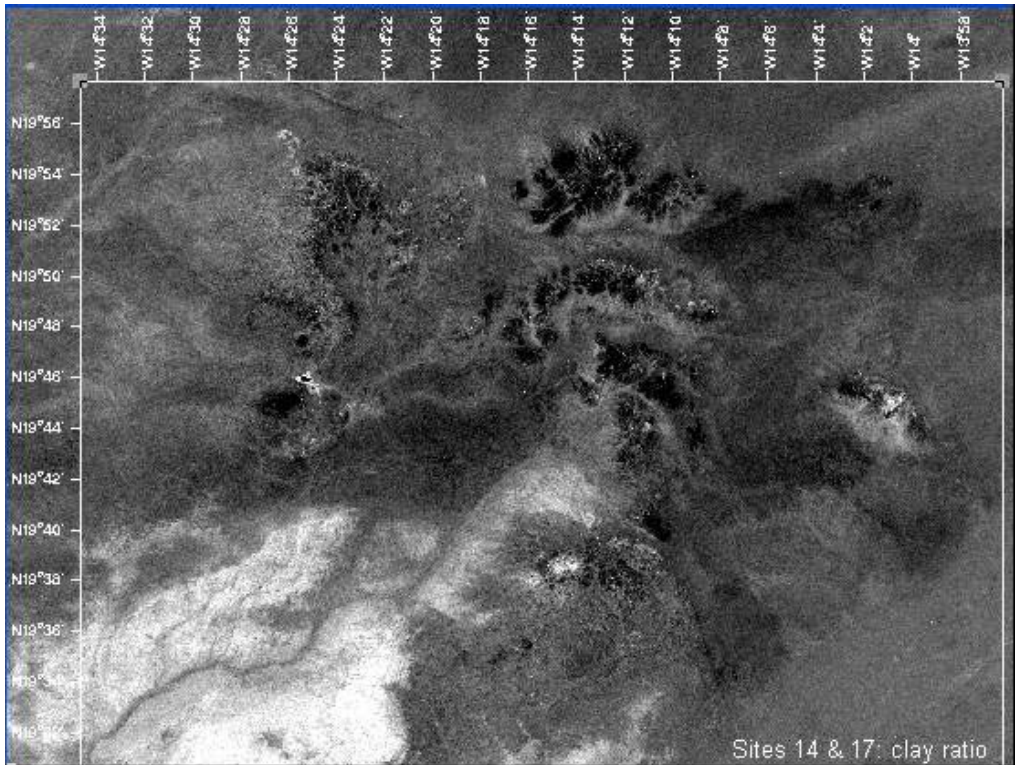


Figure 8 Clay abundance: white = maximum. No clay alteration around the Tabrinkout W anomaly; small patches of alteration around Akjoujt mine.

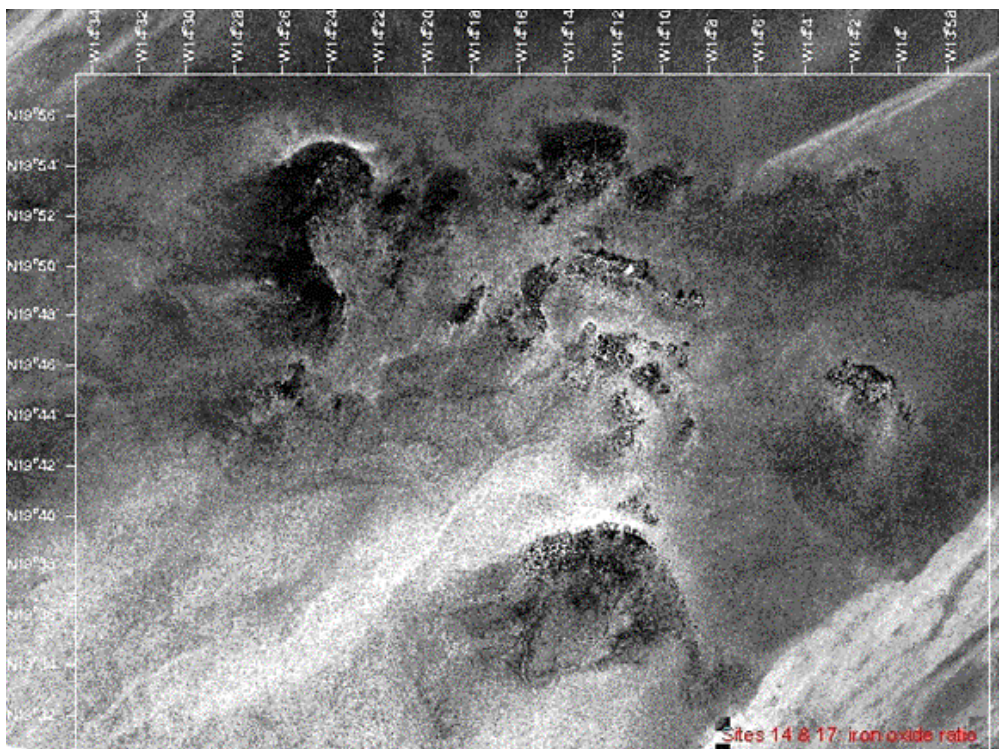


Figure 9 Fe ratio, highlighting haematite-stained dune sands and Fe-rich alluvial-colluvial sediments derived from the Banded Iron Formations, which have a speckled appearance.

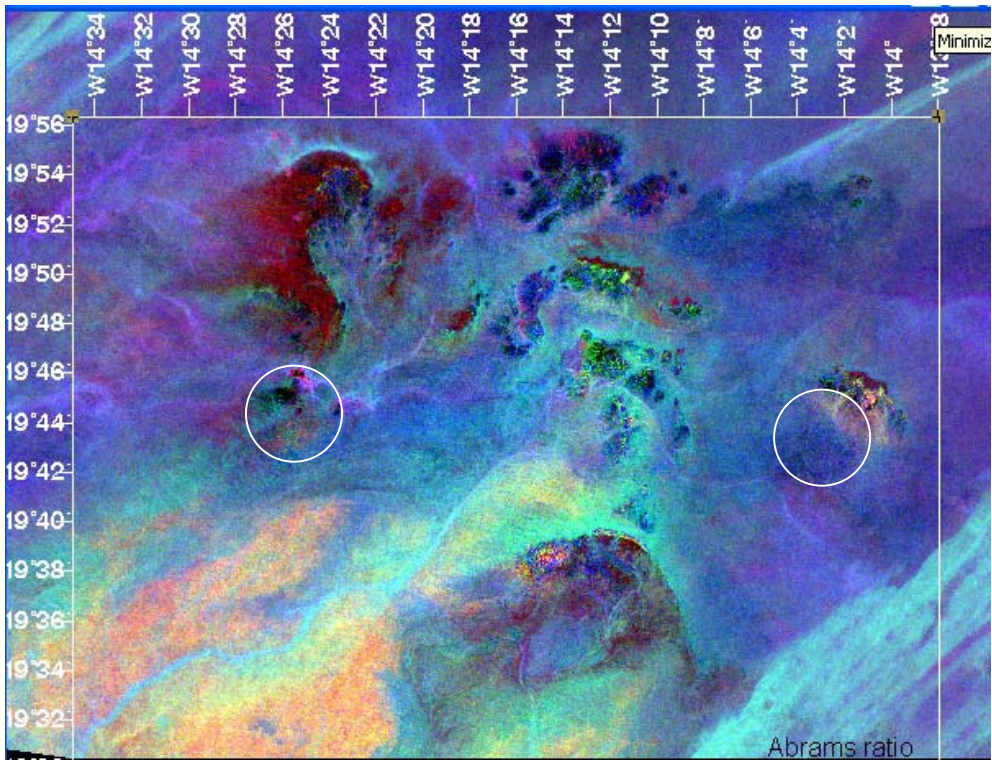


Figure 10 Abrams Ratio: clay and iron oxide abundance. Brown = hematite; yellow-red = kaolinite and iron oxides, mostly over orthogneiss; pale blue = quartz-rich; blue = schists and meta-carbonates.

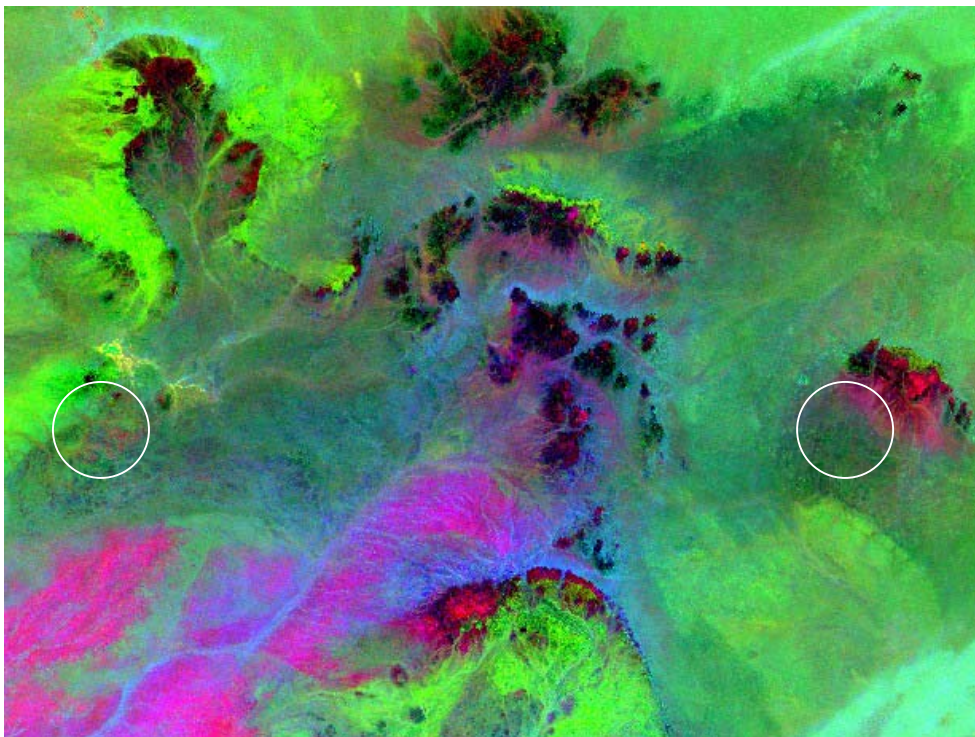


Figure 11 Complex Band Ratio ((5/7 4/5 3/1 RGB). Black-Red = BIF Pink = quartzite/orthogneiss; Dark green = chlorite schist, with dark grey lenses of meta-carbonate; grey = quartz-rich.

## 2. Zoueratet LANDSAT image processing

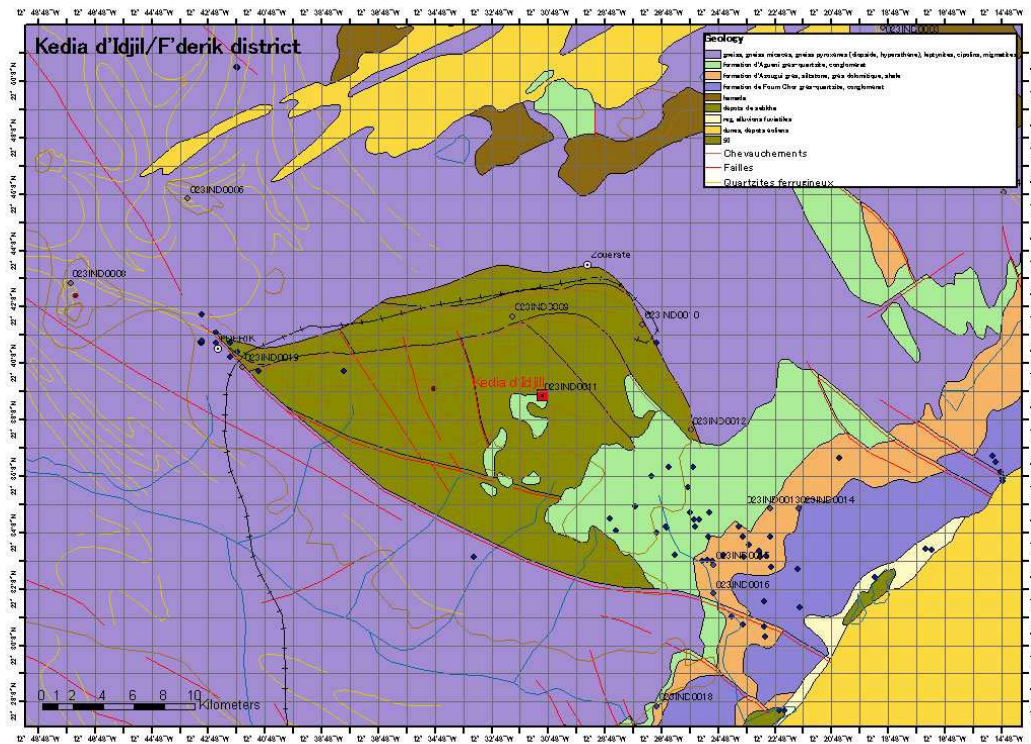


Figure 12 Geology of the F'Derik— Koedia -Idjill area (after 1:200,000 series, SIGM database)

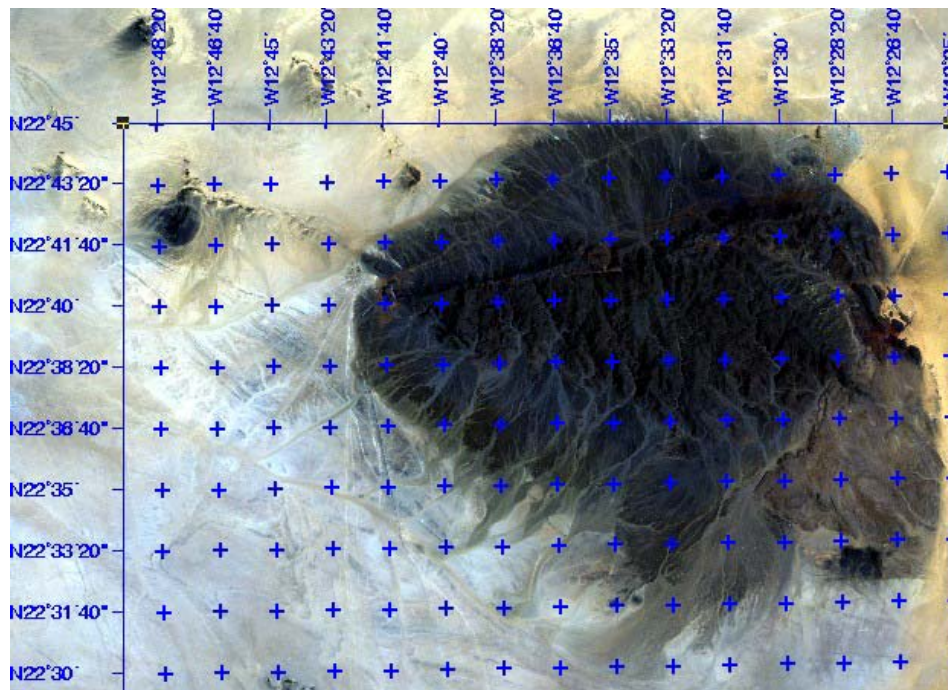


Figure 13 LANDSAT ETM false-colour infra-red image (432 RGB)

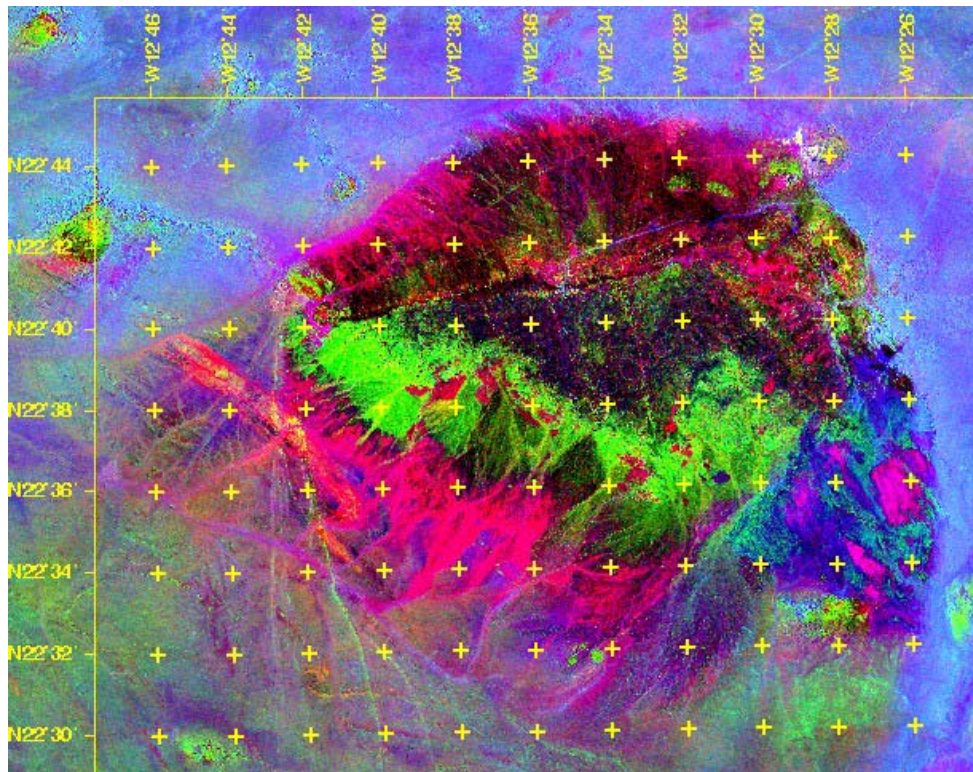


Figure 14 LANDSAT ETM: 5/7 4/3 3/1 RGB. Red-black = iron oxides / laterite  
Green = iron hydroxides; Blue = quartz-rich; Pink-blue = conglomerate.

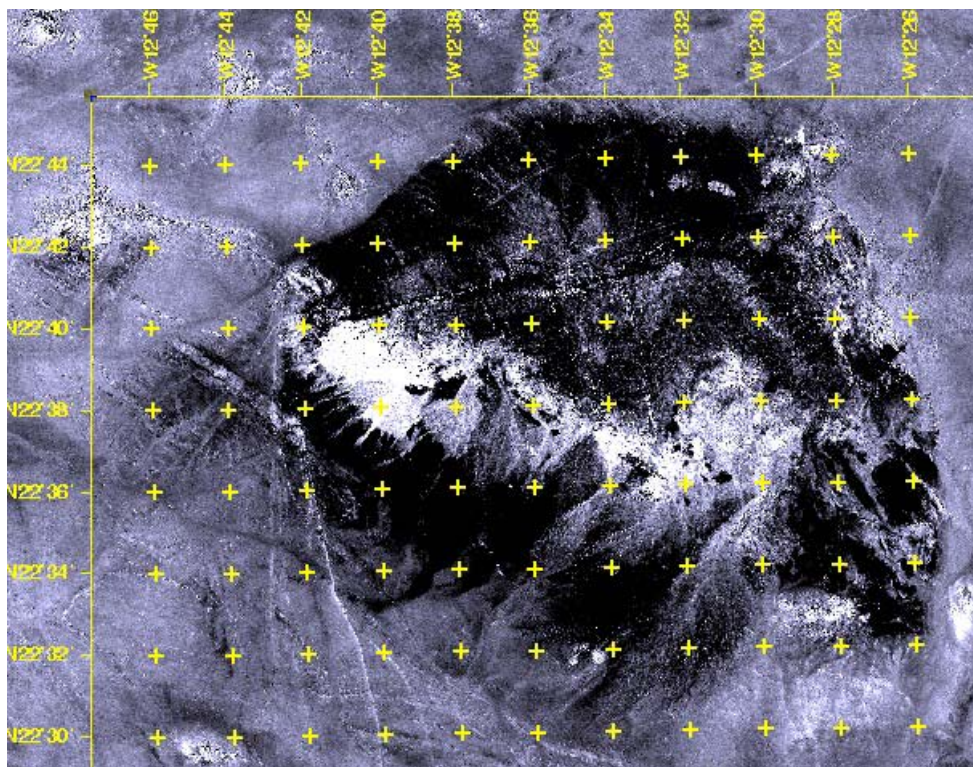


Figure 15 LANDSAT ETM 5/4 – abundance of iron hydroxides (white)



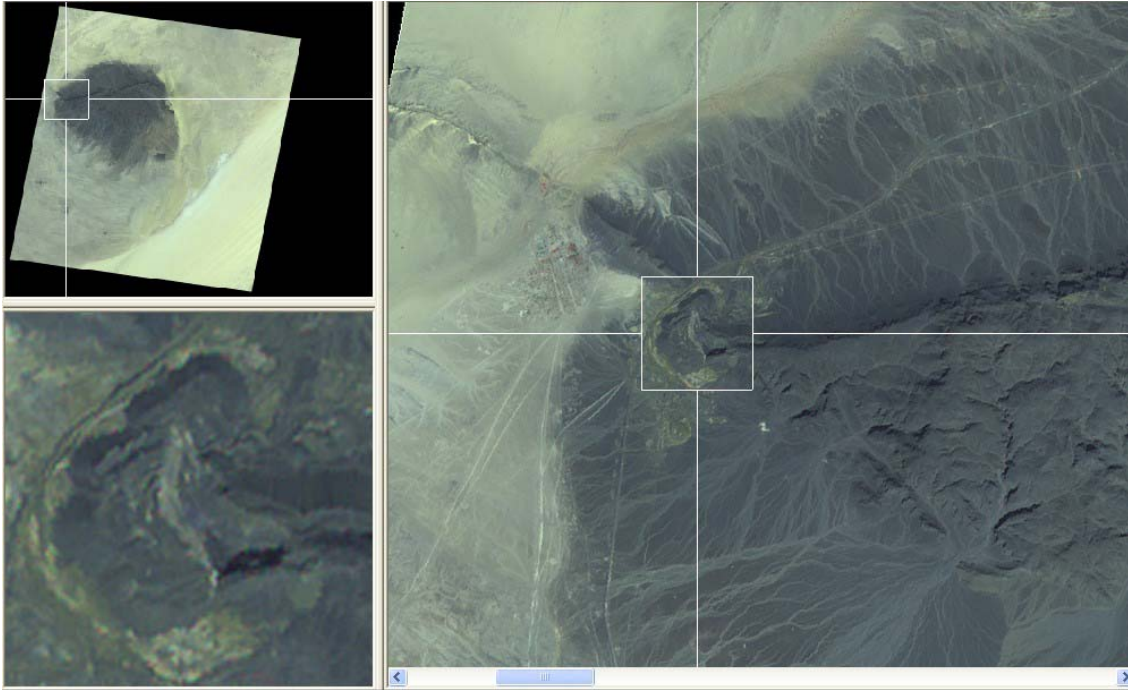


Figure 16 ASTER false-colour infra-red (321 RGB), focused on F'Derik Fe Mine.

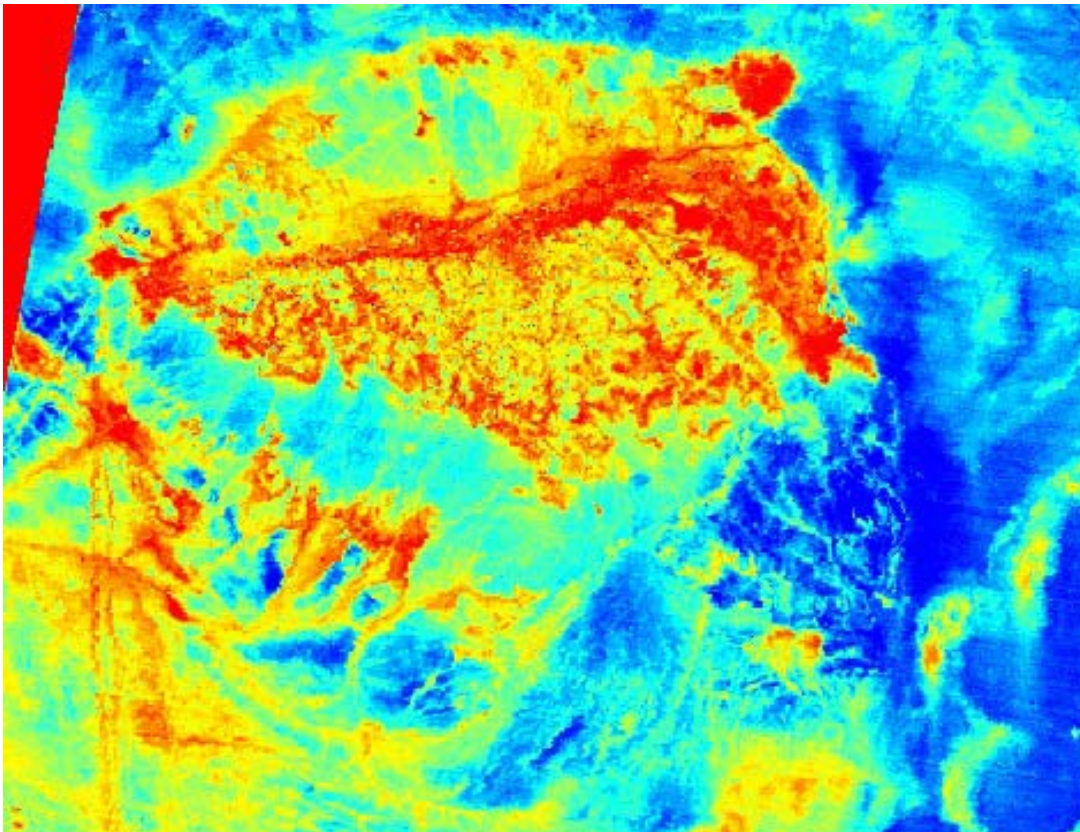


Figure 17 ASTER thermal band ratio (13/14)

### 3. Tasiast LANDSAT image processing

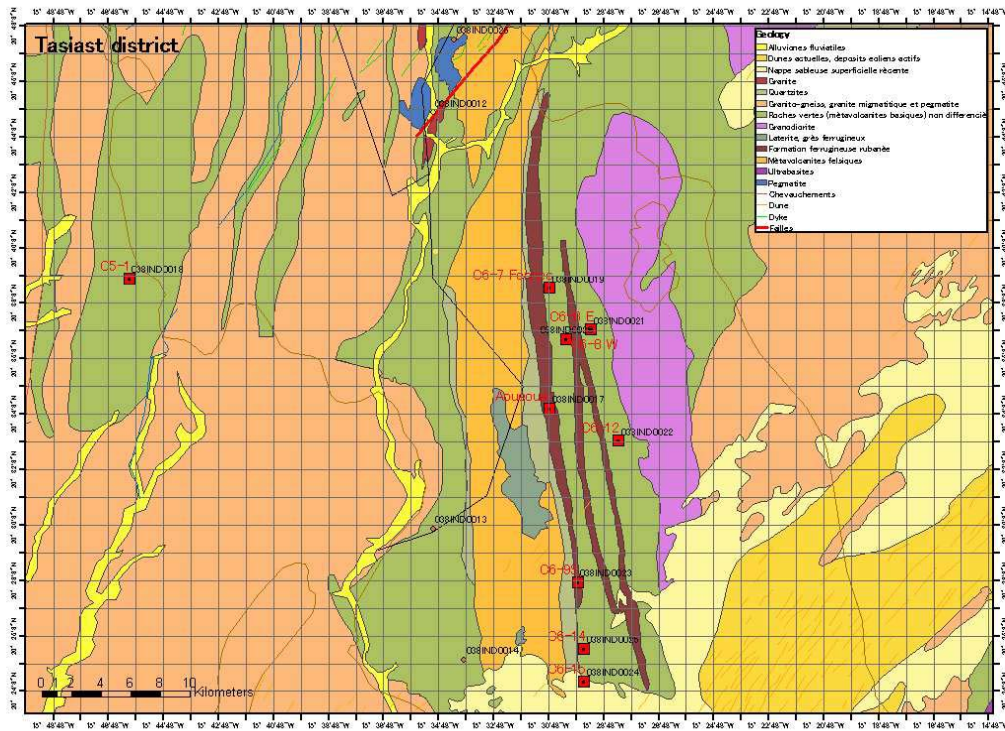


Figure 18 Geological map of Tasiast area (after 1:200,000 series, SIGM database)

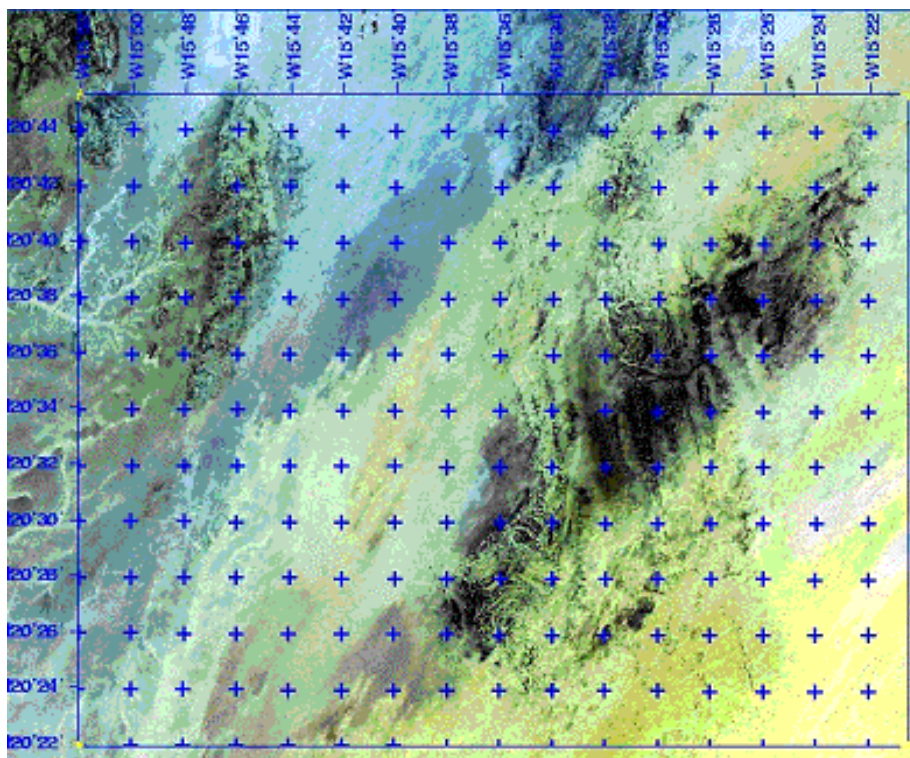


Figure 19 LANDSAT ETM 'true-colour' image of Tasiast (321 RGB)

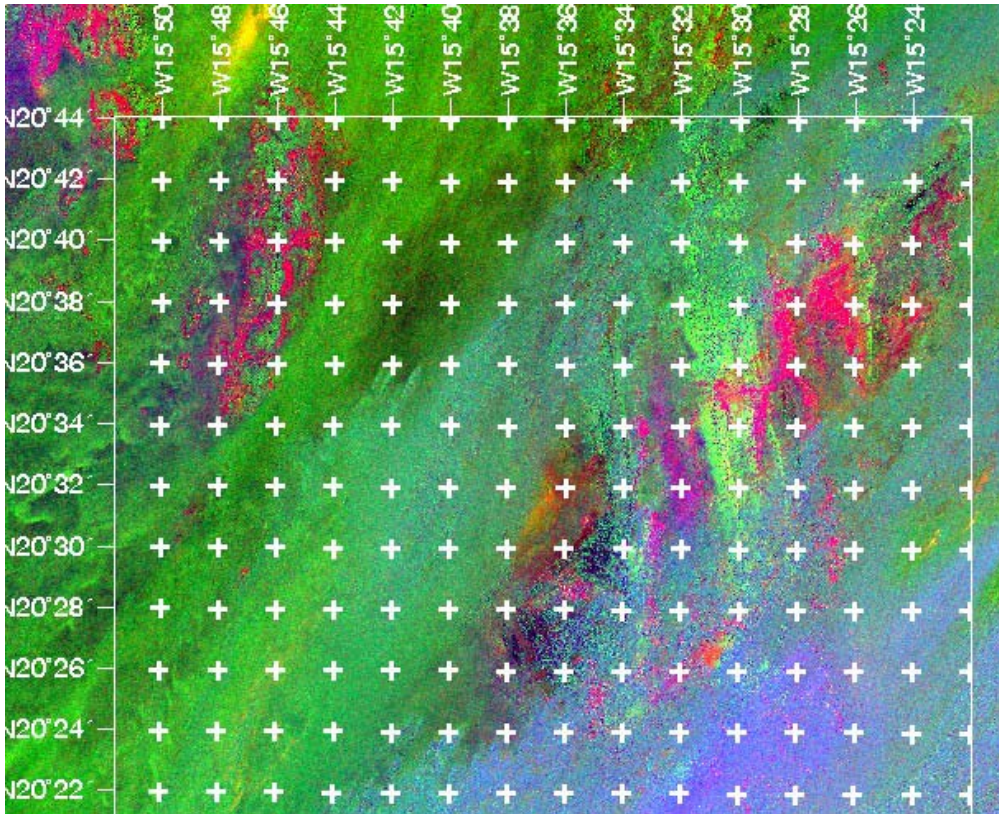


Figure 20 Tasiast - LANDSAT ETM 5/7 4/5 3/1 RGB. Dark Green = migmatite/gneiss; Blue = quartz-rich; Blue-Pink = felsic metavolcanics; Apple Green = granite; Red = Granodiorite; Red-Brown = Greenstone Belt laterite.

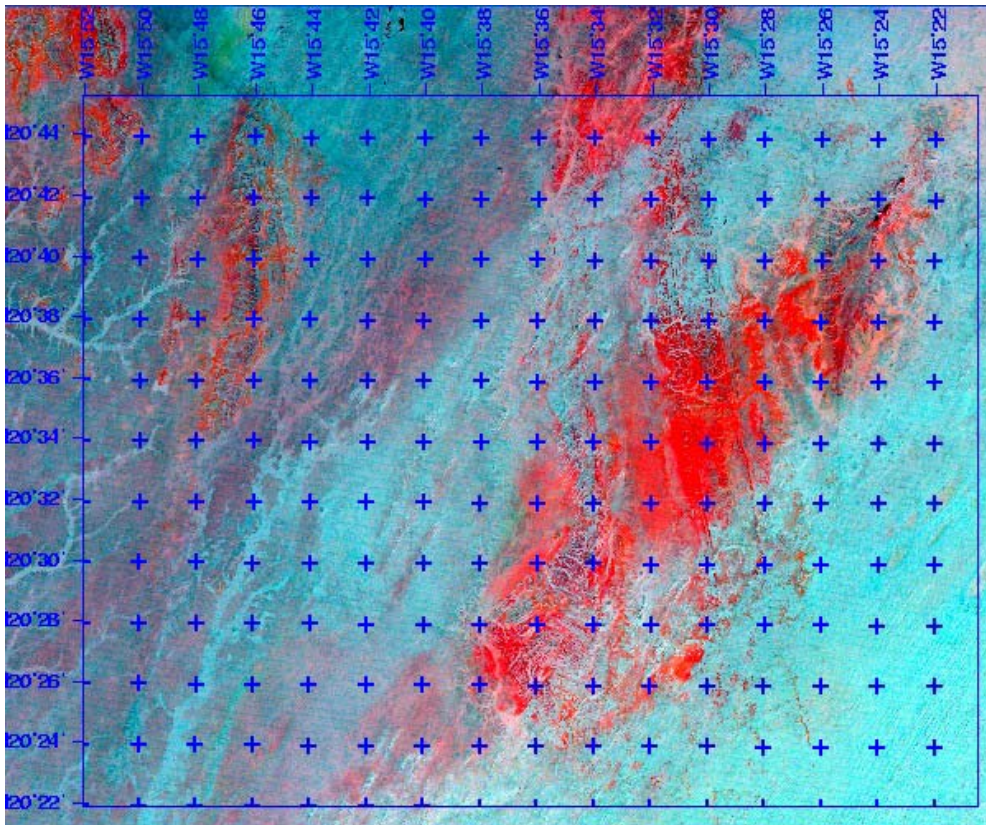


Figure 21 Tasiast – LANDSAT 657 RGB – thermal anomalies in red.

### **3.2 Remote sensing analysis**

#### **1. The Role of Remote Sensing Analysis for Mineral Resources Survey**

The role of remote sensing for mineral resources survey means analysis of geological structure and grasping of location and size of mineral resources. Mineral resources survey is divided into each stages of general survey, detailed survey, prospecting drilling and mining exploitation. It is used for remote sensing to select high potential area of prospecting in general surveying stage, extract drilling area in detailed surveying stage, to survey neighboring area of mineral deposit in the prospecting drilling stage, to monitor effect of mining and drain water in mining exploitation stage.

The practicable surface depth by remote sensing analysis corresponds to few micrometers from surface in the case of optical sensor, maximum 10 meter in the case of radar. As the reason of metallic ore deposit is able to appear relatively shallow place underground, it is useful for remote sensing as direct prospecting method.

Mainly, remote sensing analysis is separated to classification of rock or mineral and analysis of geological structure. Reflectance and radiant spectral of rock and mineral using optical sensor is the information reflected chemical composition of mineral. The other, the information using radar shows roughness of ground surface.

Porphyry copper deposit and shallow water-based gold deposit accompany with some extent alteration zone on ground surface. Remote sensing using optical sensor is useful for mineral investigation to grasp the distribution of alteration mineral. In recent years, hyper spectral resolution sensor, which has few of ten to few hundred-observation bands, put to practical use. The sensor can recognize and identify mineral.

#### **2. Data for Remote Sensing Analysis**

As for the data for remote sensing analysis, they are an observed spectrum, and information on the topographical features by the sensor carried on the satellite or the airplane. This time, it made use of satellite data because surveying period was short and survey area was vast. At present, the satellite data, which are the most effective in the mineral resources survey, are LANDSAT of the United States and an ASTER satellite by the Japanese-American cooperation.

Many data are accumulated since LANDSAT is launched by the United States as a global resources satellite in 1972. After 1984 years, 2.2 $\mu$ m (band 7) of the short infrared wavelength was added in the LANDSAT satellite with request of the resources survey user. This band, which is called Clay Band, is made effective in resources survey because it shows absorption of various clay minerals, carbonic acid salt mineral, and so on. ASTER (Advanced Space-borne Thermal Emission and Reflection) is the global resources satellite where it is launched in 1999. ASTER observes into each five bands which are infrared bands(8.125~11.65 $\mu$ m) and thermal infrared bands (2.0~2.5 $\mu$ m), so that it can precisely recognize mineral survey.

Table 2.1 shows the comparison of LANDSAT and ASTER data. The main differences are the

ground resolution and the number of observation bands. In this study ASTER data are mainly used and LANDSAT data are complemented. In the appendix, satellite data list and coverage map of satellite are shown.

Table 2.1 Comparison of LANDSAT and ASTER data

Term	LANDSAT ETM				ASTER			
Band number	8bands(Band 8:Panchromatic mode)				14 bands (except DEM)			
Wavelength				Unit (μm)				Unit (μm)
	Visible	Blue	Band1	0.45 ~0.52	VNIR	Green	Band1	0.52 ~0.60
		Green	Band2	0.53 ~0.61		Red	Band2	0.63 ~0.69
		Red	Band3	0.63 ~0.69				
	Near infrared		Band4	0.75 ~0.90	SWIR (Near infrared)	Band3	0.76 ~0.86	
			Band5	1.55 ~1.75		Band4	1.600~1.700	
			Band7	2.09 ~2.35		Band5	2.145~2.185	
				Band6		2.185~2.225		
				Band7		2.235~2.285		
Thermal Infrared		Band6	10.4~12.5	TIR (Thermal Infrared)	Band8	2.295~2.365		
					Band9	2.360~2.430		
					Band10	8.125~8.475		
					Band11	8.475~8.825		
Panchromatic		Band8	0.52 ~0.90					
Resolution	Band1~5, 7			30m	VNIR			15m
	Bnad6			60m	SWIR			30m
	Band8			15m	TIR			90m

### 3. The Spectral Characteristic of Rock and Mineral

The various minerals composed of the rock show a spectral absorption characteristic from visible band to thermal infrared band. As remote sensing analysis is enforced to use such a mineral spectral absorption characteristic, it can recognize and identify the material distributed on the surface of the earth (Fig. 3.1). The curve in this figure is refracted downward because incidence energy of the material is absorbed selectively. Generally such a characteristic is called spectral absorption.

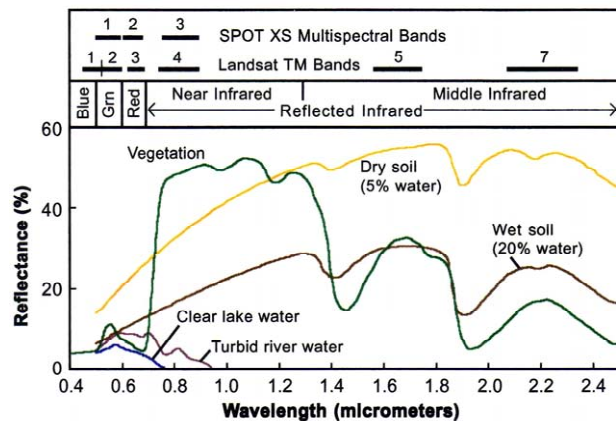


Fig. 3.1 Spectral Curve of Main Earth Surface Material. A mineral spectral absorption characteristic shows that the wavelength, which it appears in due to physics phenomenon, is different. The shape of the spectral curve and the existence of the clear absorption region or place are decided in case of a mineral by the chemical formation and the crystal

structure. The absorption of the specific wavelength occurs due to the existence of the chemical elements and the ion, the ionization elements and the existence of the chemical bond of the elements controlled by the crystal structure. The reflection spectral curve of the typical mineral is shown in Fig.3.2.

As for the spectrum of hematite, intense absorption happens in the visible band by the iron ion. It appears that absorption range continuously between 1.8~2.4 $\mu\text{m}$  in case of the calcite, which is the main element of the limestone, by existence of carbonic acid ion. Kaolinite and montmorillonite are the clay minerals contained in the soil. The absorption range, which is resistant around 1.4 $\mu\text{m}$ , is shown with both as well. The absorption, which is poor around 1.9 $\mu\text{m}$ , appears in case as kaolinite due to the existence of the hydroxide ion and. in case of montmorillonite, by the molecule of the interstitial water. On the other hand, remarkable absorption is not recognized as the orthoclase from the visible range to the middle infrared band.

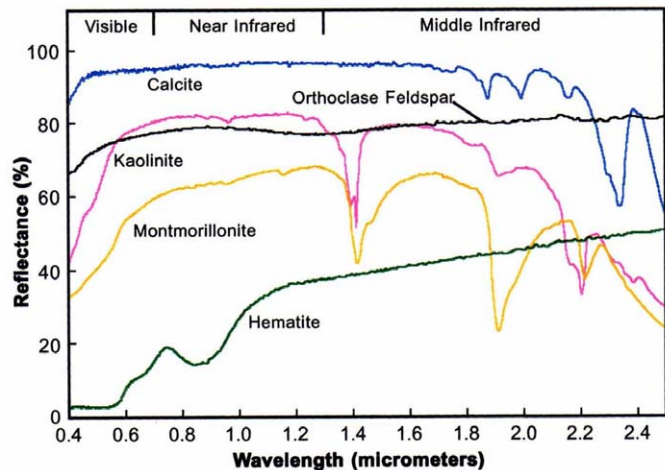


Fig. 3.2 Reflection of Spectral Curve of typical Minerals

The more detailed spectral characteristic of each bands which is divided visible band (0.4 $\mu\text{m}$ ~1.0 $\mu\text{m}$ ), short wavelength infrared band(1.0 $\mu\text{m}$ ~3.0 $\mu\text{m}$ ) and thermal infrared band(7.0 $\mu\text{m}$ ~15.0 $\mu\text{m}$ ) is shown as follows.

**(1) Visible band-near infrared band (0.4 $\mu\text{m}$ ~1.0 $\mu\text{m}$ )**

The succession metal such as Fe, Mn, Cu, Ni and Cr has the spectrum caused by the transition of the electronic energy level. The reflection spectrum of the iron oxide is shown in Fig.3.3. The most remarkable absorption in the visible to near infrared band (0.4 $\mu\text{m}$ ~1.0 $\mu\text{m}$ ) depends on charge movement between Fe-0. The reflectance of the iron oxide decreases rapidly from the blue range to ultraviolet range. The third iron absorption spectrum appears in 0.35 $\mu\text{m}$ , 0.45 $\mu\text{m}$ , 0.55~0.65 $\mu\text{m}$  and 0.75~0.95 $\mu\text{m}$ . The second iron absorption spectrum appears in 1.0~1.1 $\mu\text{m}$  and 1.8~2.0 $\mu\text{m}$ . Typical mineral reflection spectral curve of visible to infrared band is shown in Fig.3.4 as well.

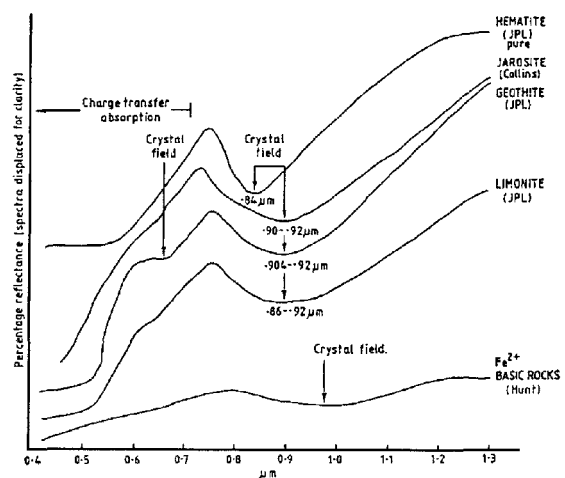


Fig. 3.4 Iron Oxide in Visible to Infrared Band

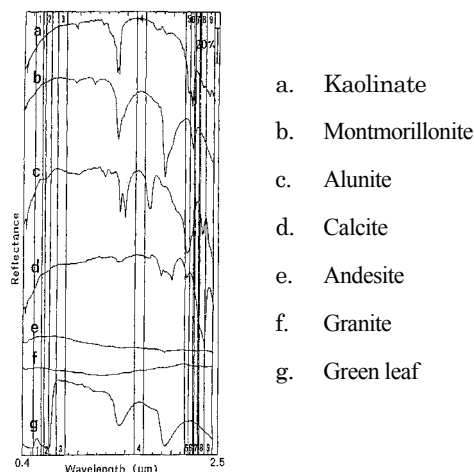


Fig.3.4 Typical mineral reflection spectral curve of visible to infrared band  
(A number 1 - 9 show the observation band of ASTER).

**(2) Near Infrared wavelength (1.0μm~3.0μm)**

As for the short infrared wavelength, the spectrum that influences vibration between the atoms, which they combined with each other, is observed. The spectrum of the vibration of combined atom appears in 2.7μm~3.0μm and 9.0μm~11.0μm. As for these spectrum characteristics, a hydroxyl, carbonic acid base, and so on influence it in the mineral component. Especially various spectra such as a clay mineral (It has an Al-OH base, a Mg-OH base, and so on.) and carbonate mineral are important.

The main element of the clay mineral resolves due to weathering of the mother rock and hydrothermal process. The material dissolved in water such as Ca and Na is leached as that result. Si and Al, Mg and Fe that it remain, are combined with water, and it forms hydro silicate material. Some of the clay minerals (in such cases as non-crystalline silicate minerals etc.) are not layer silicate minerals, but chemical composition and crystal structure are closely related to kaolin mineral and so on, which are layer-silicate minerals.

The spectral curve of the clay mineral and carbonate mineral are shown in Fig. 3.5, and Table 3.1 shows classification of mineral for near infrared wavelength. The characteristics of the spectral reflection of clay mineral and carbonate mineral are as the following.

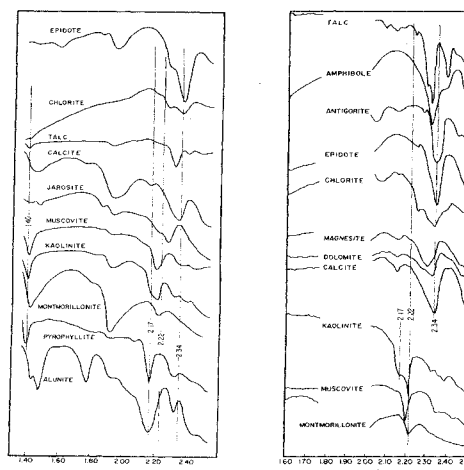


Fig. 3.5  
Various Reflection Spectrum Curves of the Short Infrared Wavelength Range of the Clay and Carbonate Mineral

- a. An absorption spectrum by the Al-OH base appears in the wavelength range of 2.16~2.24 $\mu\text{m}$ . Typical minerals are clay mineral and alteration mineral such as alunite, kaolinite, montmorillonite, pyrophyllite, white mica and illite. It thinks that the acid hydrothermal water, which forms alteration zone, raise with reacting with the rock and are neutralized gradually. Therefore the circulatory system of hydrothermal water is observed that zoning distribution of alteration mineral change of acidity of hypothermal corresponding to the change of acid content of hypothermal (silification rock  $\rightarrow$  alunite  $\rightarrow$  kaolinite  $\rightarrow$  montmorillonite  $\rightarrow$  propylite from the center).
- b. An absorption spectrum by the  $\text{CO}_3$  base appears in 2.3~2.39 $\mu\text{m}$ . There are various carbonate minerals such as calcite and dolomite in the mineral, which contains a  $\text{CO}_3$  base.
- c. The absorption spectrum by the Mg-OH base appears in 2.3~2.39 $\mu\text{m}$ . Typical mineral is in such cases as serpentine, the chlorite (three-octahedron), amphibole and blue site.
- d. The absorption spectrum by the Fe-OH base appears in 2.24~2.27 $\mu\text{m}$ . There are jarosite, nontronite and so on in the mineral, which the characteristics of the spectrum by the Fe-OH base are shown in.

Table 3.1 Classification of Mineral for Near Infrared Wavelength

Chemical Composition	Absorption Characteristic of Wavelength ( $\mu\text{m}$ )	Group of mineral	Representative mineral
Al-OH	2.16~2.24	Alunite	Alunite
		Kaolin mineral	Kaolinite, Tychite
		Pyrophyllite	Pyrophyllite
		Diocahedral smectite	Montmorillonite
		Diocahedral vermiculite	Vermiculite
		Diocahedral mica	Mica, Illite Crystallite
		Chlorite	Cokeite
		Hydro oxide minerals	Gibbsite
	Alumino silicate minerals	Sillimanite, Topaz	
	2.3~2.39	Epidote	Epidote
Mg-OH	2.3~2.39	Serpentine	Chrysotile, Antigorite
		Talc	Talc
		Triocahedral smectite	Saponite, Pectolite
		Triocahedral vermiculite	
		Triocahedral mica	Biotite, Phologopite, Clintonite
		Triocahedral Chlorite	Chlorite
		Hydro oxide minerals	Brucite
Amphibolite	Anthophyllite, Tremolite, Forblende		
Fe-OH	2.24~2.27	Alunite	Jarosite
		Diocahedral smectite	Nontronite
Si-OH	2.24	Water content silicate minerals	Opal
$\text{CO}_3$	2.3~2.39	Carbonate minerals	Calcite, Dolomite, Siderite, Magnesite
$\text{H}_2\text{O}$	2.0~2.5	Salphate minerals	Gypsum
		Zeolite	Natrolite, Heulandite, Anacite

### (3) Thermal infrared band (7.0 $\mu\text{m}$ ~15.0 $\mu\text{m}$ )

Thermal infrared wavelength range is the wavelength range which thermal radiation from ground



surface correspond the source of radiation. The spectrum, which influences a vibration between the atoms that they combined with each other, is observed in this wavelength range. The characteristic spectrum of main rock mineral is shown about the silicate mineral such as quartz, feldspar and so on in this wavelength stage.

The most important things in a mineral to distinguish in thermal infrared wavelength range are various silicate minerals. The various transparent spectrum curves of the silicate mineral are shown in the Fig.3.6 in thermal infrared wavelength range. The transparent spectral characteristic in the thermal infrared range of the typical rock is shown in the Fig.3.7.

Spectral characteristic of the silicate mineral in thermal infrared wavelength range is put together as follows.

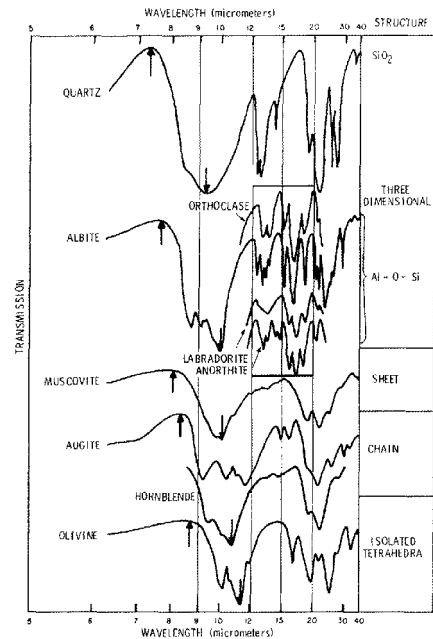
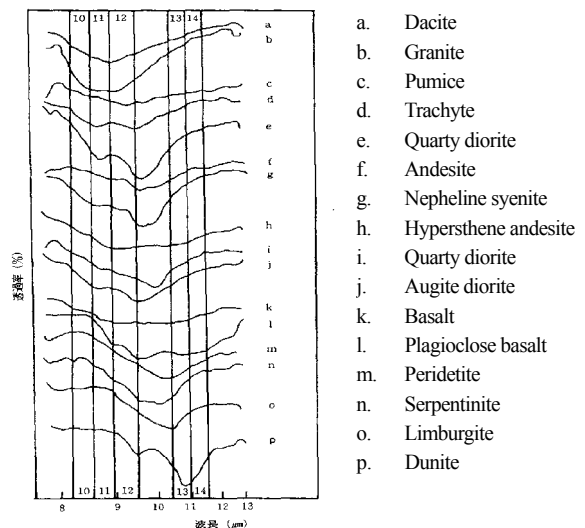


Fig. 3.6 Transparent Spectrum Curve of Silicate

- As  $\text{SiO}_2$  content decreases, the position (wavelength) of the maximum value of the emissive changes from the short wavelength side to the long wave head side in the wavelength stage of  $7.0\mu\text{m}\sim 9.0\mu\text{m}$ . In other words, maximum value shows a tendency to change from  $7.0\mu\text{m}$  (acidity) to  $9.0\mu\text{m}$  (super-base).
- The absorption spectrum to originate in the oscillation of Si-O appears in the wavelength range of  $8.5\mu\text{m}\sim 12.0\mu\text{m}$ . The wavelength that emissive is minimized, wavelength of tectosilicate, which degree of condensation of  $\text{SiO}_4$  is high, is short(the neighborhood of  $9.0\mu\text{m}$ ), and wavelength of solosilicate and nesosilicate, which the degree of condensation are low, get long as for. (nearly  $11.5\mu\text{m}$ )
- Only tectosilicate salt shows absorption spectrum in the wavelength range of  $12.0\mu\text{m}\sim 15.0\mu\text{m}$ , and other silicate minerals don't show absorption.

Fig. 3.7

Transparent spectral curve in thermal infrared wavelength range of typical rock  
Number 10 - 14 is the observation bands of ASTER.



### 3.3 List of ASTER imagery

No.	Mineral Deposit Site	Volume	Observation Date	Granule ID
1	Sfariat	1	13/10/2002	AST3A-1 021013 113053 021102 0453
2	Zouerate (Kadia & Tiris)	1	23/10/2000	AST3A-1 001023 114355 031217 1168
3		2	23/10/2000	AST3A-1 001023 114404 031217 1168
4		3	08/09/2001	AST3A-1 010908 113645 031217 1169
5		4	08/09/2001	AST3A-1 010908 113654 031217 1181
6	Tasiast (Tasiast & Tijirit)	1	23/07/2000	AST3A-1 000723 111945 041006 0911
7		2	19/09/2000	AST3A-1 000919 115752 031217 1170
8		3	19/09/2000	AST3A-1 000919 115801 031217 1171
9		4	21/10/2000	AST3A-1 001021 115656 031217 1185
10		5	21/10/2000	AST3A-1 001021 115705 031217 1182
11		6	22/02/2002	AST3A-1 020232 113855 020306 2189
12		7	22/02/2002	AST3A-1 020232 113846 020306 2188
13	Akjoujt (Taburinkout & Inchiri)	1	01/12/2000	AST3A-1 001201 114958 031217 1172
14		2	11/12/2001	AST3A-1 011211 114657 031217 1172
15	Kadiar (Kadiar & Indice78)	1	07/10/2000	AST3A-1 001007 114546 031217 1174
16		2	01/11/2003	AST3A-1 031101 113145 031217 1183
17		3	07/10/2000	AST3A-1 001007 114555 031217 1186
18		4	01/11/2003	AST3A-1 031101 113154 031217 1175
19	Diaguili (Diaguili & Guidimaka)	1	30/09/2000	AST3A-1 000930 114009 031217 1176
20		2	23/11/2002	AST3A-1 021123 112722 031217 1177
21		3		
22	Jreida-Lemsid	1	03/09/2000	AST3A-1 000903 115845 031217 1178
23		1		

### 3.4 List of LANDSAT ETM

No.	PATH	ROW	Observation date	Mineral deposit site
1	199	43	27/04/2003	
2	200	42	04/05/2003	
3	200	43	04/05/2003	
4	201	42	09/04/2003	
5	201	43	09/04/2003	
6	202	42	16/04/2003	
7	202	43	16/04/2003	
8	202	44	16/04/2003	
9	202	49	27/02/2003	Diaguili (Guidimaka & Diaguili)
10	202	50	27/02/2003	Diaguili (Guidimaka & Diaguili)
11	203	42	06/03/2003	
12	203	43	06/03/2003	Sfariat
13	203	44	06/03/2003	Kedia (kedia & Tiris)
14	203	45	06/03/2003	Kediar (kedia & Tiris)
15	203	46	06/03/2003	
16	203	47	06/03/2003	
17	203	48	06/03/2003	Kadiar (Kadiar & Indice78)
18	203	49	06/03/2003	Kadiar (Kadiar & Indice78)
19	204	44	14/04/2003	
20	204	45	14/04/2003	
21	204	46	14/04/2003	Akjoujt (Inchiri & Taburinkout)
22	204	47	14/04/2003	Akjoujt (Inchiri & Taburinkout)
23	204	48	14/04/2003	
24	204	49	13/03/2003	
25	205	45	05/04/2003	
26	205	46	05/04/2003	Tasiast (Tasiast & Tijirit)
27	205	47	05/04/2003	Tasiast (Tasiast & Tijirit)
28	205	48	05/04/2003	
29	206	45	28/04/2003	
30	206	46	28/04/2003	

### 3.5 List of Topographical Map (1:200,000)

No.	Map No.	Name of Map	No.	Map No.	Name of Map	No.	Map No.	Name of Map
4	2510	Bel guerdan	54	1910	Adofer el Abiod	80	1706	Nkhaile
5	2509	Ain Ben Till	55	1909	Hoflat Sardoun	81	1705	Zouina
10	2411	Tourassin	56	1908	Abolog	82	1616	Saint-Louis
11	2410	Glelbat	57	1907	Oumm Ahmar	83	1615	Dagana
12	2409	Tmelimichat	58	1906	Kratil	84	1614	Podor
16	2312	Oumn Dfeiret	59	1905	El Felje	85	1613	Kaedi
17	2311	Oumn Rouelssine	60	1815	Nouakchott	86	1612	Mbout
18	2310	Zednes	61	1814	Aguilal-Fal	87	1611	kiffa
19	2309	Rhall Amane	62	1813	Bir-Allah	88	1610	Tintane
23	2212	Fderik	63	1812	Ksar el Barka	89	1609	Nema
24	2211	Tourine	64	1811	Tidjikja	90	1608	Timbedgha
25	2210	Tenoumer	65	1810	Ganeb	91	1607	Hassi Touli
26	2209	Aguelt	66	1809	Tichit	92	1606	Niout
30	2112	Ohar	67	1808	Aratane	93	1605	Selibabi
31	2111	Guelb er Richat	68	1807	Kedama	94	1513	Matam
37	2016	Nouadhibou	69	1806	Aklet-Awana	95	1512	Selimane
38	2015	Chami	70	1805	Mgata Tauria	96	1511	Kankossa
39	2014	Ahmeyine	71	1715	Nimjat	97	1510	Yelomane
40	2013	Atar	72	1714	Boutilimit	98	1509	Nioro
41	2012	Chinguetti	73	1713	Aleg	99	1508	Balle
42	2011	Ouadane	74	1712	Moudjeria	100	1507	Nara
49	1915	Nouamghar	75	1711	Boumdeid	101	1506	Sege
50	1914	Akjoujt	76	1710	Tamchekket	102	1505	Nampla
51	1913	El gleltat	77	1709	Bou Derga	103	1412	Bakel
52	1912	Far aoun	78	1708	Ouftene	104	1411	kayes
53	1911	El Moinan	79	1707	Oualata			